A STUDY OF THE INFLUENCE OF HEAT TREATMENT ON FIELD EMISSION IN SUPERCONDUCTING RF CAVITIES

Q.S. Shu, W. Hartung, J. Kirchgessner, D. Moffat, H. Padamsee, D.L. Rubin and J. Sears* Laboratory of Nuclear Studies. Cornell University, Ithaca, N Y 14853, USA Received 9 May 1988 and in revised form 1 November 1988

The influence of heat treatment (HT) above 1100°C on field emission (FE) in superconducting radiofrequency (1.5 GHz) cavities was investigated. The experiments show higher average achievable fields with HT than with only a chemical treatment (CT); i.e. the average maximum surface field E_{pk} improved to 29 MV/m from 18 MV/m without taking advantage of the benefits of He processing. Using He processing, HT raised the average E_{pk} reached by cavities to 38 MV/m from the 22 MV/m achieved by a combination of CT and He processing Surface magnetic fields greater than 1000 Oe were achieved in three out of the eight heat treatment, in contrast to one out of fifteen chemical treatments. The highest surface electric and magnetic fields achieved were 50.5 MV/m and 1260 Oe respectively. If these surface electric (magnetic) fields were reached in a 5-cell accelerating structure of the same cell geometry, the accelerating field would be 20.5 (27) MeV/m at a Q of ~ 2×109. Most of the HT tests (including the record) were still limited by FE. We find that FE can be progressively reduced by He processing with increased rf power. Up to 160 W of rf power have been used during processing. A high speed/superfluid FE temperature mapping system was used to measure the power deposited by the impact of electrons emanating from field emitters. FE and defect associated heating are characterized through detailed analysis of temperature distribution maps over cavity surfaces. The maps show a greater abundance of emitters present on CT cavity surfaces than on HT surfaces.

1 INTRODUCTION

Superconducting radiofrequency (SRF) technology is finding widespreaded use in accelerators for elementary particle physics, nuclear physics and free electron lasers [1]. Major research and development efforts on super conducting (SC) cavities have been carried out at CERN, DESY, Stanford, Karlsruhe, Wuppertal, KEK, Orsay, and Cornell for many years. One of the most important aims of this research has been to achieve the highest possible accelerating fields. Multipacting and thermal breakdown, which originally limited the performance of SC cavities, have been successfully analyzed, understood, and controlled; as a result multicell accelerating structures now routinely achieve maximum surface electric fields (E_{pk}) of 12-20 MV/m with present day chemical treatment (CT) techniques. Better results are achieved in single cell test cavities: experience at Cornell has shown that E_{pk} , values of 15 to 30 MV/m can usually be reached with 1.5 GHz single cell cavities using CT. To approach a surface magnetic field at which superconductivity in Nb would break down, implies a surface electric field in the vicinity of 100 MV/m, well above the present capabilities of Nb cavities; thus there is much room for improvement.

Efforts to achieve higher fields have encountered serious problems with field emission (FE). Field emitted electrons are accelerated to 100s of keV in the high electric fields, and strike the cavity surfaces causing heating and emitting bremsstrahlung X-rays. FE of electrons from metal surfaces was first treated as a quantum mechanical tunneling phenomenon by Fowler and Nordheim (FN). From this theoretical treatment, we expect that surface fields of the order of 1000 MV/m are needed to get currents significant enough to be observable in rf cavities. However, SC cavities already show excessive currents at much lower fields, sometimes even at 10 MV/m. I-V characteristics are still found to fit the behavior predicted by FN, if one assumes that the increased emission occurs from regions where the local electric field is enhanced by a factor of β . β values between 100 to 1000 are frequently extracted from FE data [2].

It has been known for a long time that the excess FE occurs at isolated sites. Originally these sites were thought to be metallic microprotrusions (whiskers) where the field was assumed to be locally enhanced by a factor β.

^{*} Work supported by the National Science Foundation, with supplementary support from the US-Japan collaboration.

^{**} Nuclear Instruments and Methods in Physics Research A278(1989)329~338 North-Holland, Amsterdam

Recent studies in which emission sites were located by a dc probe and subsequently examined by SEM have conclusively shown that the enhanced FE is associated with anomalous, superficial particles or inclusions on the surface [3,4]. However, such features have geometrical shapes that could only exhibit β values of order 10, so that some mechanism other than geometrical field enhancement appears to be at work. Studies of the emitted electron energy spectra suggest that the sites cannot be purely metallic in nature and models basad on semiconductors and insulators seem more consistent with the observed energy spectra [5].

Substantial progress has been made on empirical characterization of dc field emitters on Nb surfaces. Typically half a dozen emission spots/cm² are seen at field levels up to 40 MV/m. Of these, more than 200 sites have been studied in detail over a surface area of 200 cm². The emitting particles have sizes ranging from 0.5 to 20 μ m, with the most probable size between 0.5 and 1 μ m. These particles were found to contain foreign elements such as S, C, Ag, W, Cu, Si, Cr and Mn [4].

Dc field emission studies also show instability features in the FE current. Of these, the most interesting is switching of emitters to a higher emissive state [5,6]. We frequently observe similar emitter switching in rf superconduting cavities;

Substantial progress has been made in reducing the number of emitters present on a Nb surface using high temperature (HT) annealing in UHV. These results indicate that HT at $T > 1200 \,^{\circ}$ C drastically reduced the density of emitters. Surfaces of $\sim 1 \, \text{cm}^2$ size which do not emit up to $100 \, \text{MV/m}$ have been repeatedly obtained by HT above $1400 \,^{\circ}$ C. This treatment makes both particles and emission disappear [4].

Encouraged by results from the U. of Geneva, we have begun to explore the effects of ultrahigh vacuum (UHV) annealing at temperatures above 1100° C as a final surface treatment in comparison with chemical treatment (CT). Work on heat treatment is also in progress at the U. of Wuppertal [7]. We have carried out tests on 1-cell, 1500 MHz high purity Nb cavities. These cavities were made from commercially available high purity niobium, further purified by solid state gettering [8] to teach RRR values of 350-400. Model calculations [9] have shown that RRR values of 300-400 are needed to avoid thermal breakdown from ~ 0.1 mm diameter "normal conducting" type defects. High RRR also improves the ability of a cavity to withstand, without thermal breakdown, the large power deposited on the walls by the impact of FE electrons. Thus the effectiveness of processing a cavity to overcome FE and reach higher fields improves with RRR.

We have used a high speed, superfluid He, thermometer based diagnostic system for detailed char- acterization of emitter densities and behavior. Temperature maps acquired during the tests harbor a wealth of information on detail properties of emitters and other lossy areas. Only representative temperature maps will be given here to correlate with the beneficial effects of HT.

In the past, heat treatment up to 1800°C [10] was used as the final surface treatment for Nb cavities, but it was not possible to clearly study how effective this treatment was for reducing FE and for allowing higher fields because of the following reasons:

- (1) Many tests were limited not by FE but by the more frequently occurring phenomena of multipacting and thermal breakdown. The spherical (elliptical) shape cure for multipacting and the high thermal conductivity cure for thermal breakdown were not yet discovered. As a result, at ~ 1.5 GHz, field values reached were usually more than a factor of 2 lower than those reported here with heat treated cavities.
- (2) Temperature mapping techniques to observe emitters and their densities were not yet developed. This work builds on the accumulated progress over the years which allows surface E fields of 15-30 MV/m. It re-examines the influence of HT on the single dominant field limitation, FE, and uses this treatment to take SC cavities to higher field levels.

2 EXPERIMENTAL DETAILS

After chemical polishing and cleaning with standard procedures, the cavities were heat treated in a UHV furnace. The furnace maintained a vacuum of a few \times 10⁻⁷ Torr at about 1200 $^{\circ}$ C by a cryopump system. One of the problems we faced with HT is that the RRR of high purity Nb drops due to absorption of oxygen into the bulk from the residual gases in the furnace. To minimize this effect, we restricted the time and treatment temperatures as shown in table 1.

Another problem was the introduction of dust into the cavity during insertion and removal from the furnace as well as from the furnace itself. To minimize this effect we took several steps:

(1) Locate the furnace inside a Class 1000 clean room environment.

- (2) Place debris baffles (Nb foil shields) at the beam tube openings when the cavity was in the furnace.
- (3) Among the first five tests, three cavities were rinsed with dust-free high purity methanol after HT. We noticed substantially less FE and higher final fields. Subsequently we routinely rinsed all cavities to remove possible particulate contaminants that could be introduced while opening the furnace and removing the cavity.

After withdrawal from the furnace, the cavities were sealed with clean polyethelene caps and transported to a Class 10 clean room, where they were rinsed and dried. End pieces with an rf coupler and pumping holes were assembled to the cavity with indium joints. The final attachment to the rf test setup was carried out in front of a Class 100 portable laminar flow unit.

During the rf tests, we utilized a high speed/superfluid FE temperature mapping system to locate and analyze the FE sources from the power deposited on the cavity surface by emitters in an rf field. In this system, 684 carbon resistor thermometers mounted on 36 boards (19 for each board) are affixed to the cavity so that each resistor is in thermal contact with the outer wall of the cavity, shown in fig. 1. This large number of fixed thermometers allows us to measure the temperature distribution faster than the older technique of mechanically moving a smaller array over the cavity surface. This system can scan the entire surface of the cavity in 15 s, as opposed to the older scanning system which takes 30 min. The high speed makes it possible to study in detail local heating as a function of field level and time. The high heat transfer coefficient of superfluid He as well as the absence of BCS losses at the low operating temperature (1.4-1.5 K) increases the temperature stability of the rf surface at high rf field. The temperature mapping system is described in detail elsewhere [11].

Table 1 List of fired cavities and the heat treatment used

	Name	Temperature[$^{\circ}\mathbb{C}$]	Time[h]	Rinsed After HT
1	LE1-21/F1	1100	2	No
2	LE1 -20	1200	2	Yes
3	LE1-12Y	1250	2.5	Yes
4	LE1-Heraeus	1350	10min	Yes
5	LE1-21/F2	1250	2.5	Yes
6	LE1-CSI/F1	1250	5	Yes
7	LE1-la	1250	2	Yes
8	LE1CSI/F	1350	15min	Yes

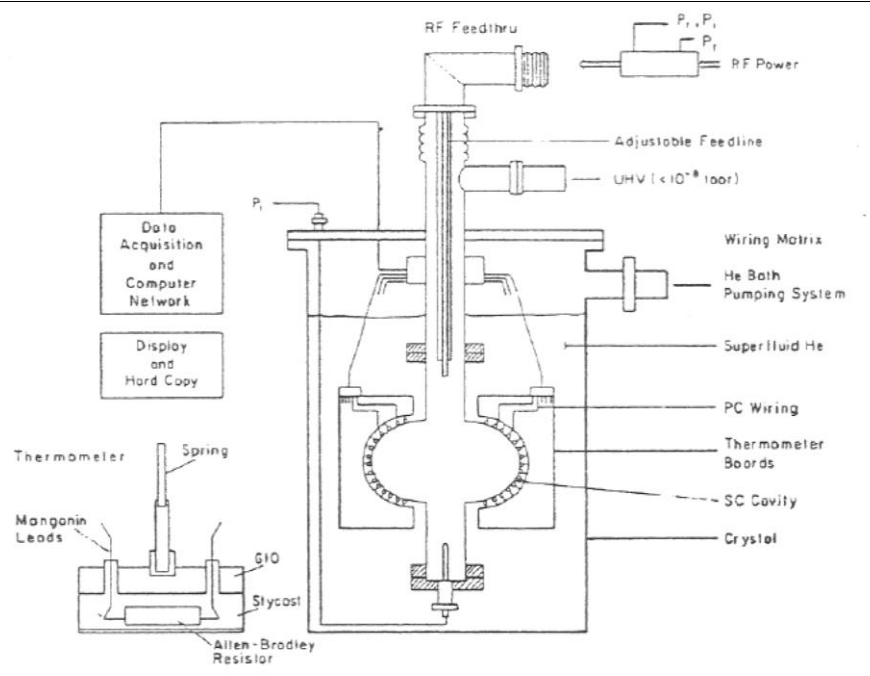


Fig. 1. Single cell, 1.5 GHz superconducting rf test cavity with superfluid He/temperature-mapping system. Each board carries 19 resistors. 36 boards are placed 10° apart.

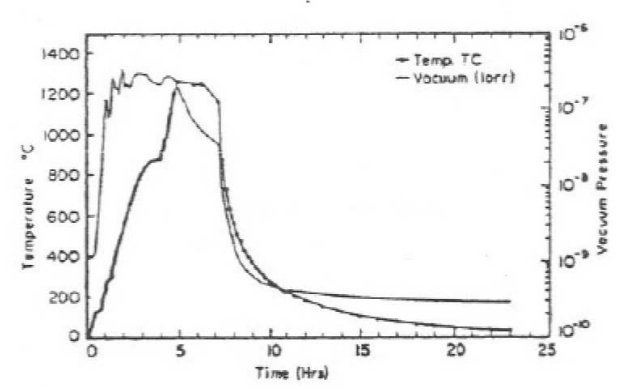


Fig. 2. Furnace vacuum behavior during a cavity heat treatment. Both temperature and pressure are shown for the entire firing cycle.

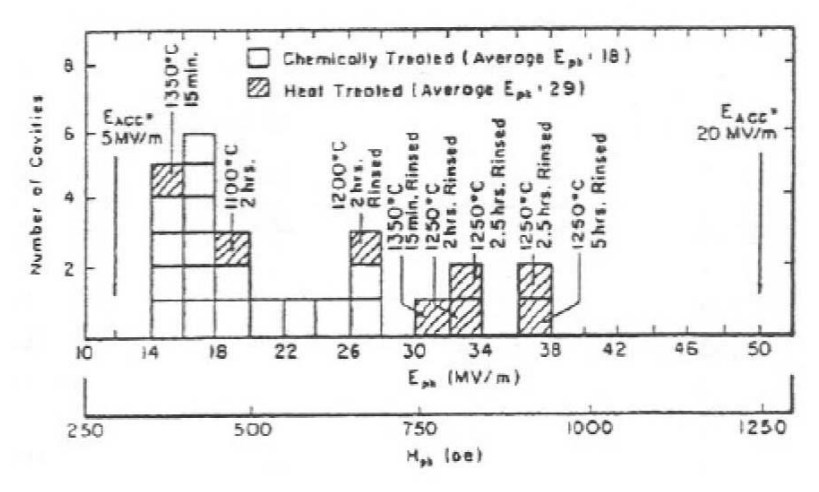


Fig 3. A statistical Comparison between the maximum E_{pk} reached by heat treated cavities and by chemically prepared cavities, without the use of He processing.

3 RESULTS AMI ANALYSIS

3. 1. Heat treatment and effect on RRR

Table 1 summarizes the details of the final surface treatments.

The O pickup is proportional to the firing temperature and duration as follows [11]:

$$\Delta C[at.\%] = \frac{1.29}{1 + 1.3 \times 10^{-2} \exp(7150/T)} \times \left(\frac{F}{V}\right) [cm^{-1}] P_{o2}[Torr] \in [s].$$
 (1)

where F/V is the surface area to volume ratio.

Fig. 2 shows the pressure and temperature vs time during a typical firing cycle. However, the pressure at the gauge does not represent the true O partial pressure in the hot zone. For this run, the O pickup estimated from eq. (1) using the assumption that all the residual gas is O, is about 11 ppm (by weight). Bulk RRR measurements on a Nb sample placed in the furnace to monitor this effect showed a RRR drop from 370 to 180, corresponding to 16 ppm pickup, in rough agreement. The true O pressure is somewhat higher than the pressure reading outside the hot zone. Results of similar experiments with other firing runs are given in table 2. From these results we conclude that it will be necessary to substantially improve the furnace vacuum before temperatures higher than $1250\,^{\circ}\text{C}$ can be used for firing cavities for several hours in out furnace.

As the BCS surface resistance at 4.2 K depends on the electron mean free path [13,14] it is possible to make a rough estimate of the surface RRR of the fired cavities from the rf resistance Table 2 gives a brief summary of our measurements of dc and rf surface RRR We note that, as expected, the surface is more heavily contaminated than the bulk.

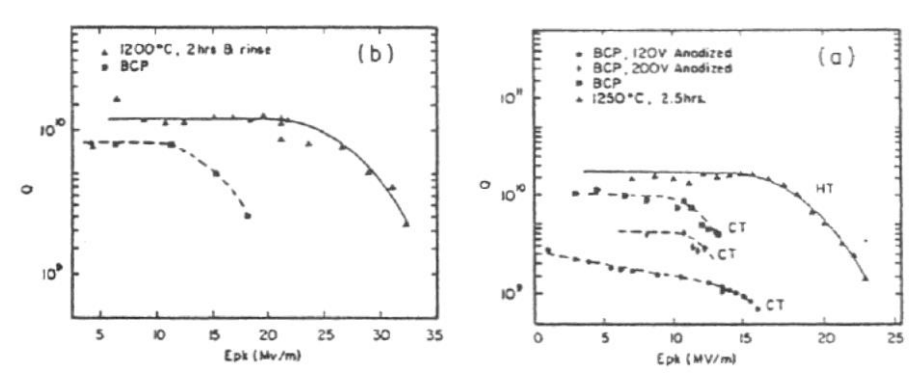


Fig. 4. Influence of heat treatment on FE loading. Each plot shows Q vs E curves for the same cavity using HT or CT, but no He processing CT cavity results are shown as dotted lines.

Table 2 The measured change of sample RRR and rf surface RRR after HT

HT condition		Rf surface RRR		Bulk sample RRR		O pickup[ppm]
T[℃]	t[h]	Before	After ^{a)}	Before	After	From sample
1100	2	400	-	-	-	
1200	2	350	150	-	-	
1250	2.5	350	170	-	-	
1350	10 min	400	100	360	250	6.7
1250	2.5	350	<100	370	180	15.7
1470 ^{b)}	2			390	60	77.6
1250	5	220	100	300	146	19.3
1250	2	400	-	290	130	24
1350	15 min	100	< 50	370	170	17.5

a)Not measured b)Only dc sample

3.2 Field emission behavior of HT cavities

In all cases but one, FE loading was still observed to be present after HT, including the phenomena of emitter switching to a high emissive state. In the exceptional case, no FE loading was detected up to 32 MV/m. Up to now, switching observed in dc studies of FE, is also a serious problem with FE in our cavities, and this remains true for HT cavities. We have discussed these phenomena in previous reports [10,14] but review the important features here for the sake of completeness. Above a threshold field level, emission at certain sites abruptly switches to a high level after the rf is kept on for some fractions of a second. The switch is accompanied by a spontaneous decrease in the cavity field level. We refer to the switching emission as state II. Before the switch, field emission is labelled as pertaining to state I. A correlated jump in the current collected by the rf antenna is also observed during switch, along with increased heating at specific locations. Even though the field decrease does reduce emission from the switched site, emission continues at a level higher than before the switch. It is usually necessary to lower the rf power level significantly below onset before switching can be arrested, and the end is accompanied by an increment in the field level. For a given switching level, the time taken to switch decreases if the incident rf power is increased in an attempt to reach a higher field in state I. β values are observed to be enhanced substantially in state II. We find that application of additional rf power in state II is sufficient to process through low field occurrences of state II. Ultimately, however, it is no longer possible to make further gains in field level with rf processing alone and a "persistent" form of state II sets in, at which point He processing

A more thorough description of state II emission will be presented in a subsequent paper.

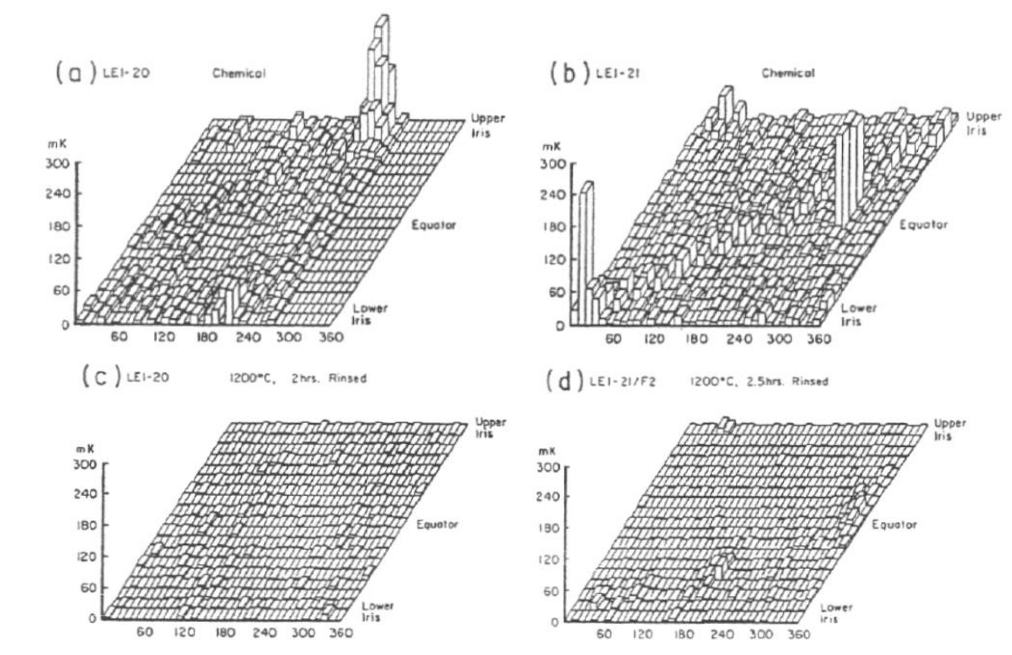


Fig.5. A comparison of temperature distribution maps at about 16 MV/m. At this field, CT cavities (a, b) showed significant FE loading that can be successfully characterized by thermometry. At the same field level HT cavities(c and d)show no emitters.

During rf tests on HT cavities, both rf processing and He processing were used in an attempt to reach the highest possible fields with the available rf power. It is well known that He processing is more effective in reducing FE emission in cavities [10]: The comparisons we make below are an attempt to ascertain whether heat treatment alone is responsible for any improvement in FE loading. We therefore give representative comparisons for the HT and CT treatments in the following ways:

- (1) The highest E_{pk} that can be reached with CT or HT after the effectiveness of rf processing diminishes completely (fig. 3).
- (2) The behavior of Q vs E_{pk} for the same cavity with CT vs HT before He processing (fig. 4).
- (3) The number of emitters that can be identified with our thermonetry system at 16 MV/m for CT and HT cases, before He processing (fig. 5).
- (4) The number of emitters present in HT cavities at 23 MV/m before He processing (fig. 6).
- (5) The highest E_{pk} that can be reached with CT or HT after the effectiveness of He processing diminishes completely (fig. 7).

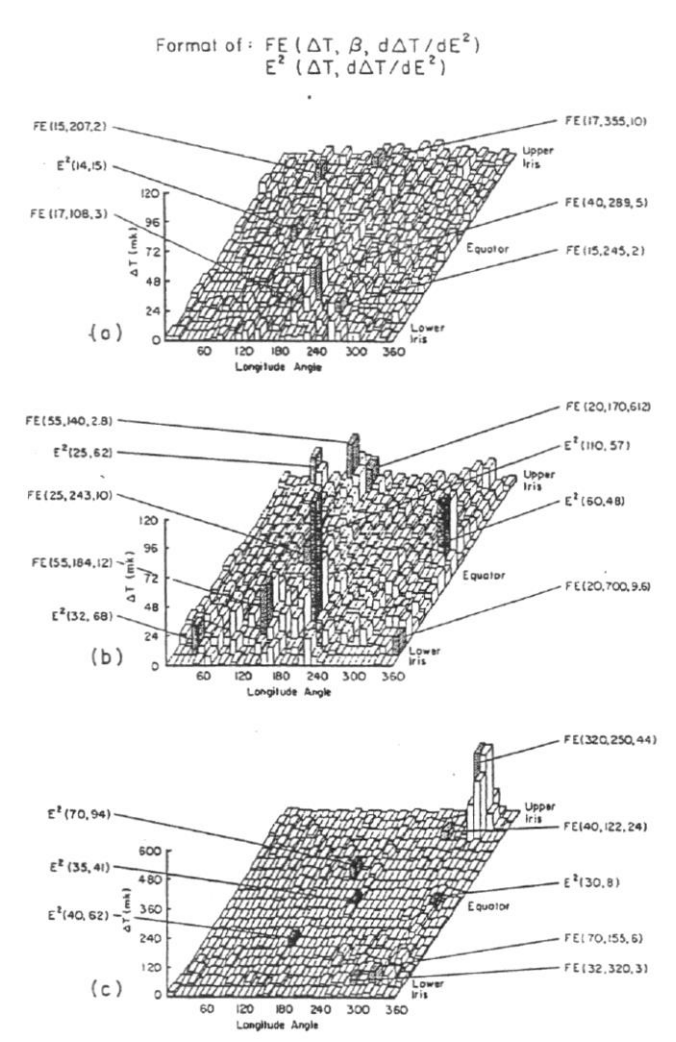


Fig. 6. The analysis of the characteristics of the main heating areas on the surfaces of the three fired cavities at an E_{pk} of 23 MV/m. without He processing. Peak heating due to emitters is shaded lightly. Emitters are labelled FE, and the values in brackets are ΔT in mK, β , and $d(\delta T)/dE^2$ in $\mu K/(MV/m)^2$ respectively. Defect heating areas are shaded dark, labelled E^2 , and the values in parentheses are ΔT and slope, $d(\Delta T)/dE^2$.

In principle, it is also desirable to compare emission between CT and HT cavities before rf processing. However, the inherent instability of emitters on first application of rf power often prevented us from acquiring systematic temperature maps during the rf processing phase.

3.2.1. Highest E_{pk} without He processing

The maximum E_{pk} reached before He processing for the fired cavities ranged from 16 to 38 MV/m; among these the better cavities had been rinsed with methanol after HT. A statistical comparison of all fired cavities with eighteen chemically prepared cavities is shown in fig. 3.

3.2.2. Q as a function of E_{pk} without He processing

A comparison of Q values between HT and CT for the two cavities is presented in fig. 4. In general, cavities show consistently lower FE loading after HT. A comparison of temperature maps (discussed below) elaborates this trend.

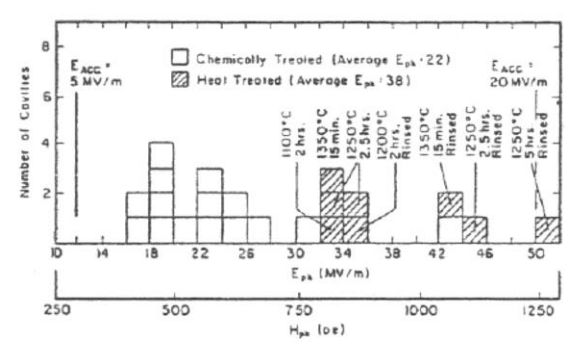


Fig. 7. A statistical comparison between the maximum E_{pk} reached by fired cavities and by chemically prepared cavities, both after He processing.

3.2.3. Comparison of FE in cavities using temperature maps at 16 M V/m

From the Q vs E behavior in fig. 4 we see that, with CT, all the cavities used in this study showed significant FE loading above 15 MV/m before He processing. Out of these tests, two were carried out after our temperature mapping system was available. In figs. 5a and 5b we present temperature maps at 16 MV/m for these two cases, showing 2-3 dominant emitters in each case. Detailed examination of heating at individual meridians showed low level emission at several additional sites, so that the total number of emitters in fig. 5a is 11 and is 6 in fig. 5b.

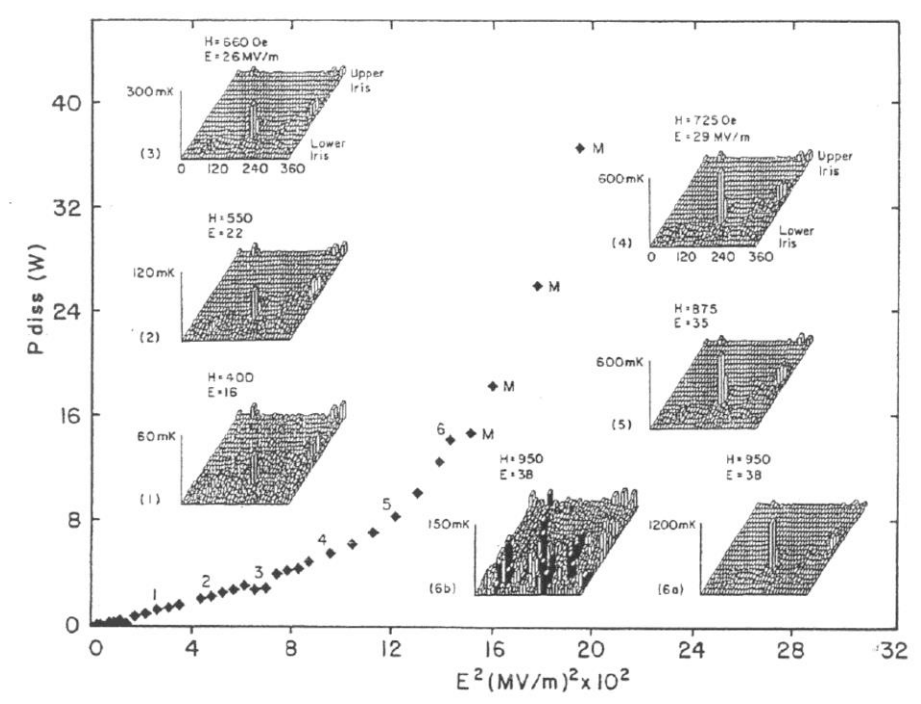


Fig. 8. Dissipated rf power for one of the best cavities after He processing to reduce emission together with accompanying temperature maps up to 38 MV/m. Defect heating dominates all maps. To see the remaining emission heating, the highest field map is also shown with expended sensitivity by artificially suppressing most areas that show defect heating. Between 38 to 45 MV/m, the rf was modulated (M) with 50% duty cycle to avoid switched emitters.

On the other hand, as expected from the reduced Q loading with heat treatment, temperature maps for the same cavities at 16 MV/m after HT show hardly any emitters (figs. 5c and 5d). Of the HT cases studied here. six cavities reached significantly higher fields than CT cavities.

3. 2.4. Temperature maps of HT cavities at 23 MV/m (no He processing)

The temperature maps for three representative cavities at 23 MV/m are shown in figs. 6a, b and c and typically show 4-5 emitters. Not all the hot spots are due to FF. Some are due to defect heating (labelled E²). The propertes of emitters (labelled FN) axe detailed in the figure. Derivation of these properties from the temperature maps is

discussed in the next section.

3.2.5. A comparison between HT and CT cavities after He processing

The highest field reached in the best cavity was 50.5 MV/m (1260 Oe) after He processing with up to 160 W of rf power. A statistical comparison between the maximum E_{pk} reached by HT cavities and by CT cavities after He processing is shown in fig. 7. The final behavior of a representative HT cavity (not the best one) after He processing is described by fig. 8 where we show the total rf dissipated power vs E^2 and accompanying temperature maps acquired at particular field levels. Above 38 MV/m, it was necessary to modulate the rf with a 50% duty cycle to avoid switching into state II emission. A defect near the equator dominates all the maps. For the highest field map, fig. 8 inset (6a), at 38 MV/m (925 Oe), we have artificially suppressed ΔT in the areas which we have conclusively identified as defect heating, and expanded the temperature scale so that the underlying emitters are visible as shown in fig. 8, inset (6b). This is one of the highest field-temperature maps we have ever recorded. A complete description of emitters present in these tests including the ones that switch and ones that subsequently process will be presented in forthcoming reports.

3.3. Analysis of the characteristics of heating sources

Temperature distribution maps make it possible to analyze the detail properties of heating sources. Heating sources on the inner surface of a superconducting cavity can be broadly categorized into two types. One type of heat source is caused by rf power dissipation at localized defects on the surface. This heating is proportional to the square of the local field. We refer to this as E^2 heating, although the actual heating mechanism may involve a combination of H^2 and E^2 . The other kind of heating is due to power deposition by the field emitted current, which we will call FN heating [2]. The emitter current can be expressed approximately as

$$I = \frac{AS\beta^2 E^2}{\phi} exp\left(-B\frac{\phi^{3/2}}{\beta E}\right)$$
 (2)

where I is in A/cm², E is in V/cm, ϕ is in eV (4 eV for Nb), A = 1.54×10⁻⁶, and B= 6.83×10⁷, S is the emissive area (cm²) and β is the field enhancement factor. By plotting $\ln(I/E^2)$ versus I/E, β and S can be obtained from the slope and the intercept of the fitted straight line. For completeness it should be noted that expression (2) ignores image charge effects. The temperature difference ΔT between superfluid He and cavity wall is proportional to the power density deposited by the impacting electrons. Following previous work [15,16], we have calculated the trajectories followed by the field emitted electrons and the deposited power density distribution. By smearing the power deposited on the inner wall to simulate heat flow through the Nb wall, we have also calculated the expected shapes for temperature maps. These shapes agree very well with experimental temperature maps and show that the peak heating takes place near the emitter [11,15]. Thus the approximate emitter location is obvious from the ΔT -map. From the "calculated" ΔT -maps, we find that ΔT also follows a FN behavior, i.e., $In(\Delta T/E^2)$ is linear in I/E, with a slope approximately (~20%) equal to the β value used for the emitter. Thus β values can be determined from Δ T-maps acquired at increasing field levels. Determining the equivalent of the emissive area in the FN picture from the maps is more difficult. The typical thermometer response is calibrated in a separate setup against a known deposited power [11]. A detailed comparison between the calculated and observed ΔT -map must be made to take properly into account the effect of trajectory dynamics. We have only carried out this full procedure for a few emitters.

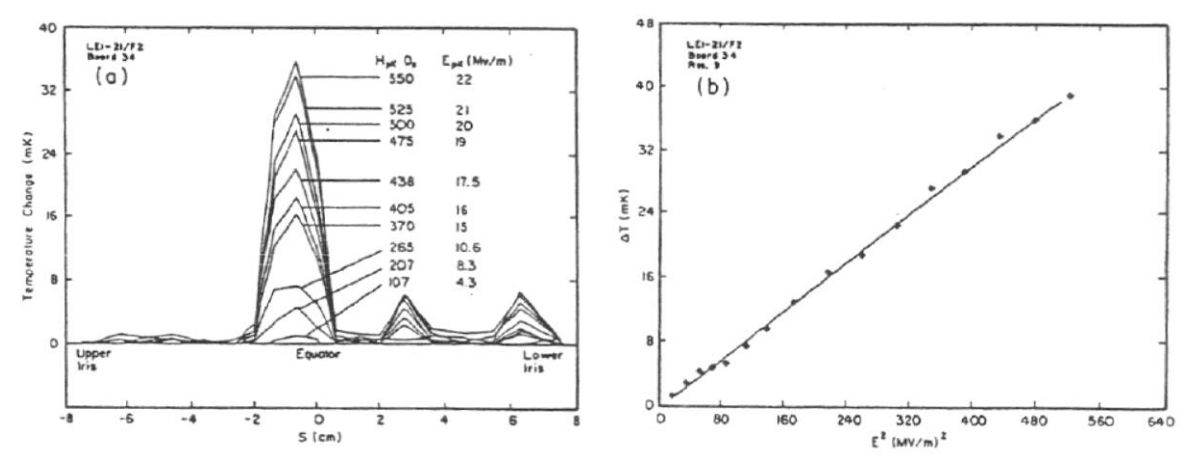


Fig 9. Typical defect heating. (a) Temperature change along a fixed longitide with increasing field E_{pk} . (b) Peak temperature change for the above defect as a function of E^2_{pk} , showing the expected linear behavior of a fixed resistance.

3.3.1. E^2 heating

Fig. 9 shows typical local heating at a lossy area near the equator of the cavity (high H region). The linear behavior of ΔT in E^2 is characteristic of heating caused by defects. The slope of the line, $\sim 70~\mu K/(MV/m)$,can be interpreted as a "resistance" for the defect. In principle, we can examine the heating at all 684 thermometers at low fields where FN heating is not significant. From the slope $d(\Delta T)/d(E^2)$ we extract a "resistance" distribution for the entire surface. This forms useful technique to characterise the residual resistance distribution over the cavity surface. As we wish to focus here on field emission results, we will present this aspect of our work elsewhere.

3.3.2 FE heating

Use of a temperature mapping technique to locate and analyze emission sources has been well established [15]. By the symmetry of the cavity and the TM010 mode, electrons emanating from an emission source are confined to impact the cavity wall at the same longitude as the source. The pattern of temperature rise caused by the impinging electrons can be used to extract information on the location and properties of emitters by comparison with simulation calculations of the electron trajectories in the cavity rf field. A new and very useful feature of our rapid temperature mapping diagnostic system allows us to track emission heating at one longitide over several increasing field levels as shown in fig. 10a for a typical emission source. The peak temperature rise is nonlinear in E², i.e. nondefect-like, and follows a FN behavior as shown in fig. 10b. However, at sufficiently low fields where we expect emission heating to be insignificant, we observe a linear region corresponding to dielectric or resistive losses. The true FE heating is obtained by subtracting out the linear component due to the other losses.

The FN enhancement factor, β , which characterizes one property of an emission source, cas be derived from a plot of $\text{In}(\triangle T/E^2)$ vs 1/E. Subtraction of the linear E^2 heating background influences the determination of β as shown by the dashed line in fig. 10c. The analysis procedure described above can be used to study the emitters in detail. A few resentative examples of the cavities are shown in figs. 6a, b and c.

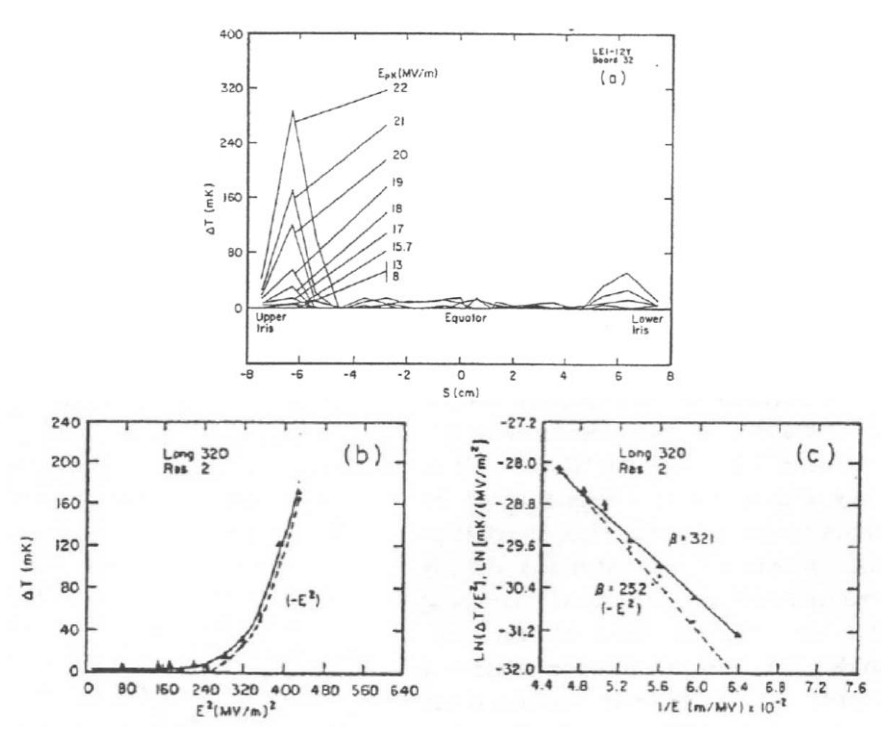


Fig. 10. Typical field emission heating. (a) Temperature change at various E_{pk} along a meridian which contains a FE heating area. (b) A plot of temperature change, ΔT , as a function of E_{pk}^2 at an emission heating area. Solid line presents the raw data. dashed line presents the same data aftex the E^2 heating component is subtracted. (c) The calculated FN enhancement factor, β . Solid line is from experimental data; dashed line is from data after E^2 is subtracted.

4 CONCLUSION

We have focussed this study on addressing one of the most interesting questions regarding FE in rf cavities: Does heat treatment reduce emission and permit higher fields, as suggested by the U. of Geneva dc FE experiments? Other important components of the FE studies have included efforts to identify the source of emitters and their detail properties investigate He processing emitter switching and role of condensed gases. The results of these studies will be given in subsequent reports.

Comparing the behavior of the fired tests with the behavior observed in preceding unfired tests on the same cavities, we observe that a higher field could be reached in the fired tests before field emission loading became intense ($Q < 2 \times 10^9$). Best results were obtained by HT between 1200 to 1250°C for ~ 2 h,followed by rinsing with methanol. Comparison of the emission landscapes revealed by the high speed thermometry diagnostic system showed that emitter density is substantially reduced after heat treatmenc This study then confirms that the beneficial effects of heat treatment observed in dc FE studies do indeed translate to a reduction in FE for rf cavities. However, emission is not eliminated.

To consistently reach surface fields higher than 24 MV/m with heat treated cavities, He processing continued to prove effective. In eight consecutive fired cavity tests, surface electric (magnetic) field values be-

tween 32-50.5 MV/m (775-1260 Oe) could be reached. For a multicell accelerating structure with the same cell geometry, $E_{pk}/E_{acc} = 2.5$ and $H_{pk}/E_{acc} = 47$ Oe/(MeV/m), so that the surface electric (magnetic) fields reached in the tests discussed here would allow accelerating fields of 13 to 20 (17 to 27 MeV/m). In most cases maximum fields were still limited by heavy FE after switching, followed by frequent trips of our radiation monitoring system. Thus higher fields can be reached by applying He processing to fired cavities, although the effect of HT up to 1250° C does not eliminate emission as hoped for. This suggests that to make further progress, higher annealing temperatures or longer annealing periods may be necessary, but it will first be important to improve the vacuum in the furnace hot zone to maintain a high RRR.

ACKNOWLEDGEMENTS

Heat treatment of 1.5 GHz cavities and the high speed/superfluid temperature map system was made possible by the dedicated efforts of the following people in design, construction and operation of the Cornell UHV furnace and map system: J. Brawley, C. Dunham, T. Giles, Y. Guy, P. Kneisel, G. Muller, R. Noer, C.Reece and the support of Cornell technician and machine shop personnel. K. Gendreau made significant contributions to many phases of this study. Sincere thanks are given to many colleagues at CEBAF, CERN, Cornell DESY, KEK, University of Geneva, and University of Wuppertal for many fruitful discussions.

REFERENCES

- [1] Proc. 3rd Workshop on R.F Superconductivity, Vols. 1 and 2 (ANL-PHY-88-1) ed. K. Shepard, Argonne, Illinois, USA (1997).
- [2] R. Noer, Appl Phys. A28 (1987) 1.
- [3] P. Niederman et al., J. Appl Phys. 59 (1986) 892.
- [4] F. Niedermann, Thesis no. 2197, University of Geneva(1986).
- [5] K. Baylias et al., Proc. Roy. Soc. Lond. A403 (1986) 285.
- [6] RV. Latham et al., J. Phys, D: Appl. Phys. 19 (1986) 699.
- [7] G. Muller, Proc. 13th Int. Symp. on Discharge Electrical Insulation in Vacuum, Paris (1988).
- [8] H. Padanmsee, IEEE Trans. Magn. Mag-21 (1985) 1007.
- [9] H. Padamsee, IEEE Trans. Magn. Mag-19 (1983) 1322.
- [10] C. Lyneis, Proc. Workshop on RF Superconductivity, ed. M. Kuntze, Karlsruhe., FRG (1980) p. 119.
- [11] H. Padamsee et al, Proc. IEEE Particle Accelerator Conf., vol. 3, Washington DC, USA (1987) p. 1824.
- [12] G. Horz, Metall. Trans. 3 (1972) 3069.
- [13] H. Padamsee IEEE Trans. Magn. Mag-21 (1985) 149.
- [14] J. Halbritter. Z. Phys. 238 (1970) 466.
- [15] H. Padamsee et al., ref. [1], p. 251.
- [16] W. Weingarten, Proc. 2nd Workshop on RF Superconductivity, vol. 2, ed. K. Shepard, CERN, Geneva, Switzerland(1984) p. 551.